Enhancing PMSG Wind Turbine Performance: A Comparative Assessment of Vector and Backstepping Control Techniques

Fadila Tahiri*‡, Abdelkader Harrouz*, Mohamed Amine Hartani*, Ilhami Colak*, Abdessalam Badoud***, Virgil Dumbarava***

* Department of sciences and Technology, Laboratory LDDI-Adrar University, Algeria.

** Department of Electrical & Electronics Eng, Istinye University, Istanbul.

*** Department of Technology and Sciences, Automatic Laboratory University of Setif 1, Algeria.

(fad.tahiri@univ-adrar.edu.dz, abd.harrouz@univ-adrar.edu.dz, ami.hartani@univ-adrar.edu.dz, badoudabde@yahoo.fr, v_dumbrava@yahoo.com)

‡Department of sciences and Technology, Laboratory LDDI-Adrar University, Algeria, Tel: +213668034483,

fad.tahiri@univ-adrar.edu.dz

Received: 23.07.2024 Accepted:30.10.2024

Abstract- This paper compares vector control (VC) and backstepping control (BC) techniques for wind systems with permanent magnet synchronous generators (PMSGs). PMSGs offer high efficiency and compact size but require advanced control strategies for optimal performance. The study evaluates transient response, tracking accuracy, robustness, and disturbance rejection. Simulations of a comprehensive mathematical model demonstrate VC's improved dynamic response and efficiency through control variable decoupling, while BC excels in tracking performance and robustness using a systematic backstepping approach. The findings aid in selecting suitable control strategies for wind energy systems and contribute to the development of improved algorithms for wind power generation.

Keywords Wind Turbine, PMSG, vector control, backstepping control.

1. Introduction

The field of renewable energy has witnessed remarkable growth in recent years, with wind power emerging as a prominent and sustainable source of electricity generation [1]. Permanent Magnet Synchronous Generators (PMSGs) play a crucial role in wind energy conversion systems, as they offer numerous advantages such as high efficiency, compact size, and improved power density [2]. However, ensuring optimal performance and stability of PMSG-based wind systems remains a significant challenge, necessitating the development of advanced control strategies [3].

In this context, the present paper focuses on the comparative analysis of two prominent control techniques: vector control (VC) and backstepping control (BC) [14]. These control strategies have been widely employed in various industrial applications due to their effectiveness in achieving accurate and robust control [15].

Vector control, also known as field-oriented control (FOC), is a well-established technique that enables independent control of the rotor flux and torque in PMSGs. By decoupling the control variables, VC provides enhanced dynamic response, reduced torque ripple, and improved efficiency. It achieves this through the transformation of the stator currents into a rotating reference frame aligned with the rotor flux [8,9].

On the other hand, backstepping control is a nonlinear control approach that has gained significant attention in recent years due to its ability to handle complex, highly dynamic systems. It employs a systematic "backstepping" procedure, where the states of the system are stabilized one by one by designing appropriate controllers [12]. This technique offers excellent tracking performance, robustness against parameter uncertainties, and disturbance rejection capabilities [13]. The primary objective of this paper is to compare and evaluate the performance of VC and BC techniques when applied to PMSG-based wind systems. The comparison will be based on several key performance

metrics, including transient response, steady-state tracking accuracy, robustness against parameter variations, and disturbance rejection. To accomplish this, a detailed mathematical model of the wind system with PMSG will be developed, incorporating the dynamics of the turbine, generator, power converter, and associated control loops. Both vector control and backstepping control algorithms will be implemented and simulated using MATLAB SIMULINK tools. A comprehensive set of simulations will be conducted under various operating conditions and system perturbations to assess the performance of each control strategy. The results of this study provide valuable insights into the strengths and limitations of vector control and backstepping control techniques in the context of PMSG-based wind systems.

Nomenclature

electromagnetic power (W).	P_{em}
Electric pulsation (rad/s).	ω
number of pole pairs.	p
rotor moment of inertia.	J
pitch angle (°).	β
tip-speed ratio (-).	λ
Mechanical generator speed (rpm).	Ω_g
Mechanical turbine speed (rpm).	$\Omega_{aér}$
permanent magnet flux (Wb).	φ_f
friction coefficient.	f
mechanical torque (N.m).	T_g
stator resistance and stator inductance of(d,q) (H).	L_d, I_d
the variable of the Laplace transform.	s
d-q axis stator current (A).	I_d, I_q
d-q axis stator voltage (V).	V_d, V_q
d-q axis flux (Wb).	φ_d, φ_q
Stator resistance (Ohm).	R_s
Controller parameters.	K_d, K_q, $K_{\Omega g}$

2. Modelling Of Wind Turbine System

2.1. *Modelling of Wind Turbine*

The kinetic energy of an air column of length dx (m), section A (m2), air density ρ (kg / m³), and wind speed v (m / s) is [4];

$$dEc=(\rho\ A.d.x.v^2\ /2) \quad (1)$$

The power coefficient Cp determines the proportion of power collected by a genuine wind rotor:

$$Pm= (Cp\ (\lambda).\rho.S.v^3\ /2) \quad (2)$$

$$\lambda = (\Omega aér.Rt)/v \quad (3)$$

Here, $\Omega_{aér}$ is rotational speed (rad/sec) and R is blade radius (m). The power coefficient has been calculated using particular readings obtained from a wind turbine by the following analytical equation [7]:

$$C_P = f(\lambda,\beta) = C_1\left(\frac{C_2}{\lambda_i} - C_3\beta - C_4\right)exp\left(\frac{-C_5}{\lambda_i}\right) + C_6\lambda \quad (4)$$

$$\frac{1}{\lambda_i} = \frac{1}{\lambda + C_7\beta} - \frac{C_8}{\beta^3 + 1} \quad (5)$$

C1	C2	C3	C4	C5	C6	C7	C8
0.5176	116	0.4	5	21	0.0068	0.08	0.035

2.2. *Modeling of PMSG*

Model of the PMSG in a frame of (d, q) axis, associated to the rotor flux vector, taking into account the hypothesis commonly considered in the modelling of alternating current machines, are [5, 6]:

- Electrical equation

The electrical equations are stated as follows:

$$\begin{cases} V_d = -R_s \cdot I_d - L_d\dfrac{dI_d}{dt} + L_q\omega \cdot I_q \\ V_q = -R_s \cdot I_q - L_q\dfrac{dI_q}{dt} - L_d\omega \cdot I_d + \varphi_f\omega \end{cases} \quad (6)$$

- Magnetic equation

Using the relationship between flows and currents:

$$\begin{cases} \varphi_d = L_d \cdot I_d - \varphi_f \\ \varphi_q = L_q \cdot I_q \end{cases} \quad (7)$$

- Mechanical equation

$$J\frac{d\Omega_g}{dt} = T_g - T_{em} - T_f \quad (8)$$

- Electromagnetic equation

$$T_{em} = \frac{3}{2}p\left[(L_q - L_d)I_d \cdot I_q + \varphi_f \cdot I_q\right] \quad (9)$$

$$P_{em} = T_{em}.\Omega_g \quad (10)$$

3. Vector Control (FOC) Of PMSG

The control of the oriented flux is a technique that introduces a method of decomposing the stator current vector into two components; one controls the flux and the other acts on the torque. The idea is to solve the problem of coupling between the two axes (d, q), where the torque is controlled by component (Iq), while the flux is controlled by (Id). By controlling the quantities (Id and Iq) acting directly on the voltages Vd and Vq [10].

In this control technique Id = 0, since it is constant, therefore the electromagnetic torque is directly proportional to Iq.

The machine model in the Park's reference is;

$$\begin{cases} V_d = R_s \cdot I_d + L_d \dfrac{dI_d}{dt} \\ V_q = R_s \cdot I_q + L_q \dfrac{dI_q}{dt} \end{cases} \rightarrow \begin{cases} V_d = I_d.(R_s + sL_d) \\ V_d = I_q.(R_s + sL_q) \end{cases} \quad (11)$$

Where; s; the variable of the Laplace transform.

- Current regulators

From (11), the expressions for the currents are;

$$\begin{cases} \dfrac{I_d}{V_d} = \dfrac{1}{(R_s + sL_d)} \\ \dfrac{I_q}{V_q} = \dfrac{1}{(R_s + sL_q)} \end{cases} \quad (12)$$

As a result, we have two comparable PI regulators that are employed in two independent loops to control the component of the axes (d, q), as shown in fig.1.

- Speed control

The dynamics of the speed is demonstrated in equation 8.

The wind speed transfer function is written as;

$$\Omega_g = \frac{T_g - T_{em}}{J.s + f} \quad (13)$$

To maintain the corresponding speed, the variable speed regulator determines the reference current Iq and the reference torque. The regulator output is a control signal which indicates the reference current Iq. The proposed control is explicated in "Fig. 1" [11].

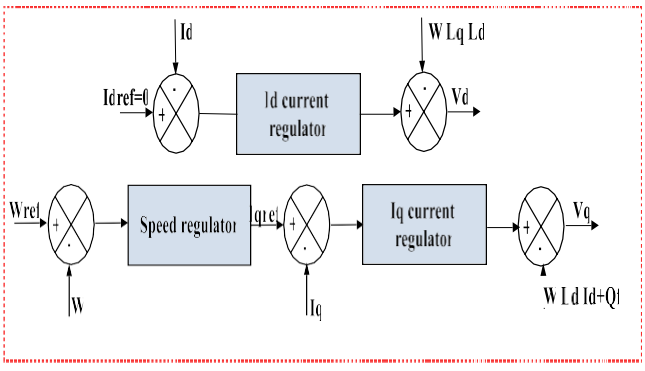

Fig. 1. Control principal diagram [15].

4. Backstepping Control

The equation (6) model is used to model PMSG. Because of the connection between current and velocity, the model has substantial nonlinearity. Backstepping control's core principle is to make the system flow in a first-order cascade stable subsystem in the sense of Lyapunov, giving it resilience and global asymptotic stability. The goal is to control the speed by using the dId/dt and dIq/dt expressions as subsystems and the stator currents as intermediate variables (Id, Iq). We can then compute the voltage commands (Vd, Vq) that are required to assure the PMSM's (Permanent Magnet Synchronous Machine) speed control as well as the overall system's stability. The expressions included here aim to elucidate the nature of the errors identified [14]:

$$\begin{cases} \xi_d = I_d^* - I_d \\ \xi_q = I_q^* - I_q \\ \xi_{\Omega_g} = \Omega_g^* - \Omega_g \end{cases} \quad (14)$$

- step1: Backstepping speed controller

speed error dynamics:

$$\dot{\xi_{\Omega_g}} = \dot{\Omega_g}^* - \dot{\Omega_g} \quad (15)$$

$$\dot{\xi_{\Omega_g}} = \dot{\Omega_g}^* - \frac{1}{J}\left[T_g - \frac{3p}{2}\left((L_d - L_q).I_d.I_q + I_q.\varphi_f - f.\Omega_g\right)\right] \quad (16)$$

In the first step, by the Lyapunov functions (eq15) a virtual control is created to ensure that the system converges towards its equilibrium state [12, 15]:

$$V_1 = \frac{1}{2}.\xi_{\Omega_g}^2 \quad (17)$$

The first derivation of Lyapunov function:

$$\dot{V_1} = \xi_{\Omega_g}\dot{\xi}_{\Omega_g}$$

$$= -K_{\Omega_g}.\xi_{\Omega_g}^2 + \frac{\xi_{\Omega_g}}{J}\left(-T_g + f.\Omega_g + K_{\Omega_g}.J.\xi_{\Omega_g} + \frac{3p}{2}.I_q.\varphi_f\right)$$

$$+\frac{3p}{2J}.(L_d - L_q).I_d.I_q.\xi_{\Omega_g} \quad (18)$$

With $\dot{V_1} < 0$. This corresponds to selecting the stator current values, Id and Iq, correctly.

$$\begin{cases} I_d^* = 0 \\ I_q^* = -\dfrac{2.J}{3.p.\varphi_f}\left[-K_{\Omega_g}.\xi_{\Omega_g} - \dot{\Omega_g}^* - \dfrac{T_g}{J} - \dfrac{f}{J}.\Omega_g\right] \end{cases} \quad (19)$$

We will replace the elements of equation (19) in equation (18) with $\dot{\Omega_g}^* = 0$:

$$\dot{V_1} = -K_{\Omega_g}.\xi_{\Omega_g}^2 \leq 0$$

- Step2: Backstepping voltage controller

In this step, the control voltages statorique in Park axis Vd (Direct voltage) and Vq (Quadratic voltage) will be calculated based on the virtual entrances of the system. A new Lyapunov

function based on the velocity tracking error and current component error to find the stator voltage references [13, 16]:

$$\begin{cases} V_2 = \frac{1}{2}.\left(\xi_d{}^2 + \xi_q{}^2 + \xi_{\Omega_g}{}^2\right) \\ \dot{V}_2 = \xi_d.\dot{\xi}_d + \xi_q.\dot{\xi}_q + \xi_{\Omega_g}.\dot{\xi}_{\Omega_g} \\ = -K_{\Omega_g}.\xi_{\Omega_g}{}^2 - K_d.\xi_d{}^2 - K_q.\xi_q{}^2 \end{cases} \quad (20)$$

Using the previous equations, we get;

$$\begin{cases} \dot{\xi}_d = \frac{1}{L_d}(R_s.I_d - p.\Omega_g.L_q.I_q - V_d) \\ \dot{\xi}_q = \frac{2}{3.p.\varphi_f}\left(\left(K_{\Omega_g}.J - f\right)\left[C_g - f.\Omega_g - \frac{3p}{2}\left((L_d - L_q).I_d.I_q + I_q.\varphi_f\right)\right]\right) \\ + \frac{1}{L_q}(R_s.I_q + p.\Omega_g.L_d.I_d + p.\Omega_g.\varphi_f - V_q) \\ \dot{\xi}_{\Omega_g} = \frac{1}{J}\left[-K_{\Omega_g}.J.\xi_{\Omega_g} - \frac{3p}{2}\varphi_f.\xi_q - \frac{3p}{2}.(L_d - L_q).I_q.\xi_d\right] \end{cases} \quad (21)$$

The control laws ultimately take the following forms:

$$\begin{cases} I_q^* = -\frac{2.J}{3.p.\varphi_f}\left[-K_{\Omega_g}.\xi_{\Omega_g} - \dot{\Omega}_g^* - \frac{C_g}{J} - \frac{f}{J}.\Omega_g\right] \\ V_d = -L_d\left(-K_d.\xi_d - \frac{R_s}{L_d}.I_d + \frac{L_q}{L_d}.I_q.\omega\right) \\ V_q = -L_q\left[-K_q.\xi_q - \frac{3.p.\varphi_f}{2.J}.C_{aér} - \frac{\varphi_f}{L_d}.\omega - \frac{L_d}{L_n}.I_d.\omega - \frac{R_s}{L_n}.I_q\right] \end{cases} \quad (22)$$

5. Simulation Results

The simulation model of wind conversion system with different control was created using the MATLAB/Simulink program.

We will undertake two parameter increases that are subject to change over time: the resistances Rd and Rq (assuming generator heating over time) and the inductances Ld and Lq (assuming saturation) as shown in (fig.3.a, b).

Table 1. Parameter of the WECSs.

Rd, Rq	*0.5(Ω)*
Ld, Lq	*0.016(H)*
Multiplier gain G	*1*
ρ	*1.2255(kg.m3)*
φ_f	*0.148Wb*
P	*17*
f	*0.001 (N.s/rad)*
J	*0.021(kg.m2)*
S	*Π.R2(m2)*

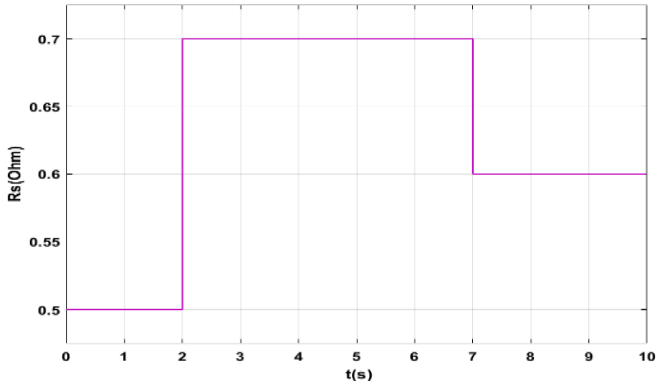

Fig.2. (a). Variation of stator resistances (Rd, Rq).

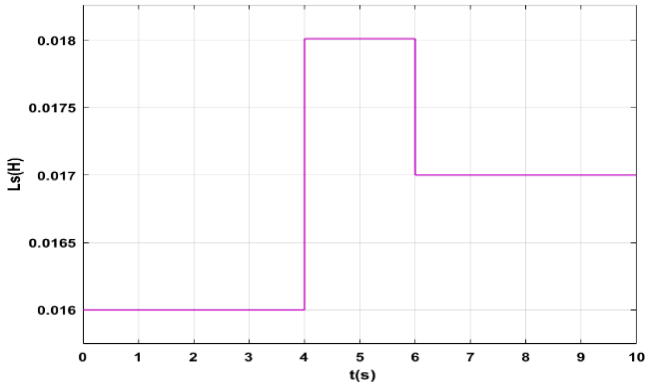

Fig.2. (b). Variation of stator inductances (Ld, Lq).

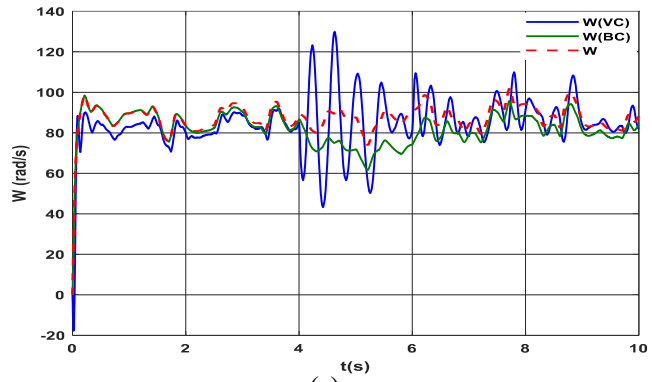

(a)

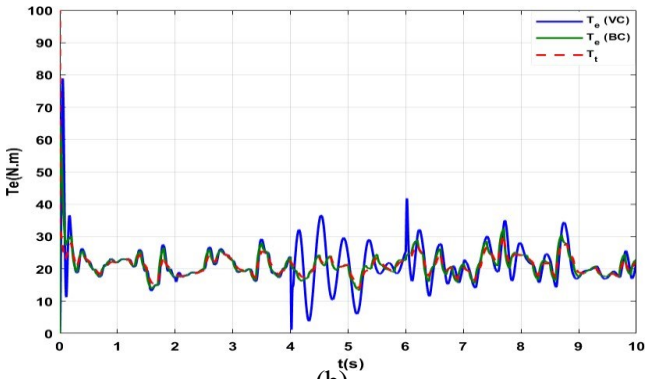

(b)

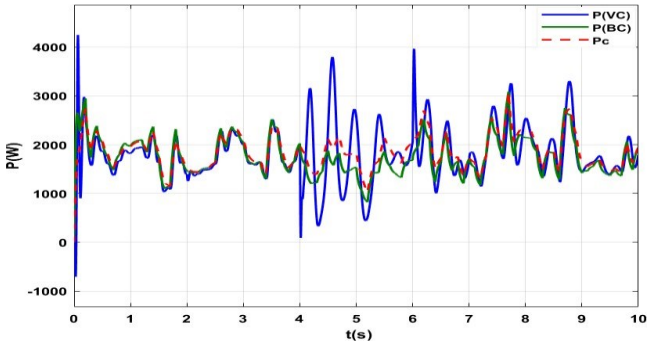

(c)

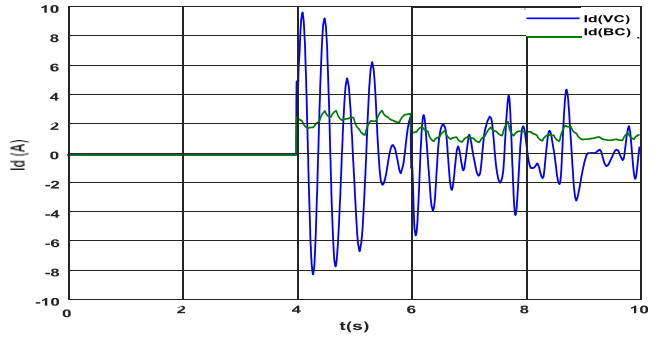

(d)

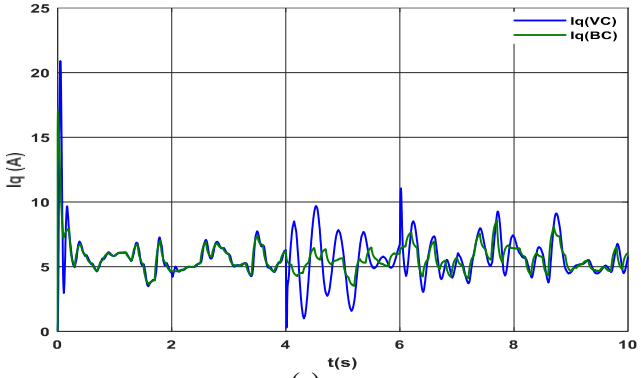

(e)

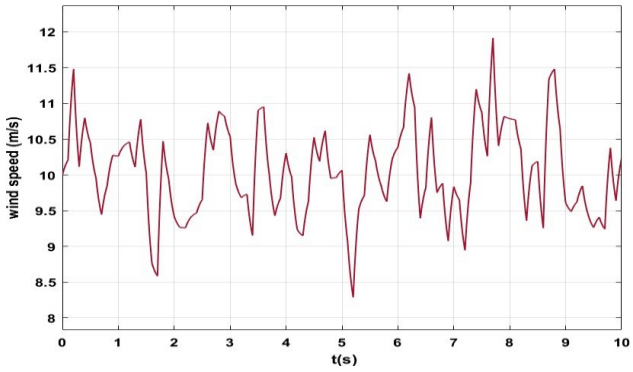

(f)

Fig.3. The different control under variations of stator parameter (R, L) (a) rotation speed, (b) electromagnetic torque, (c) power generated, (d) stator current Id, (e) stator current Iq, and (f) wind speed.

Figure 3 a, Figure 3 b, and Figure 3 c present the speed, power, and torque profiles, respectively. It is worth noting that in vector control, there is a slight initial offset in the speed and power profiles compared to the reference value, but the backstepping control accurately follows the set point. In terms of current Id (Figure 3 d), it remains at zero during operation without any applied constraints. Considering the effect of constraints (Figure 3) at t=2 seconds, where R increases by 40%, we observe no significant impact on the system. However, at t=4 seconds, when L increases by 12.5%, the vector control exhibits noticeable oscillations around the reference value in both speed (Figure 3 a) and power (Figure 3 b). The electromagnetic torque (Figure 3 c) also shows a deterioration in tracking. Similarly, the current Iq (Figure 3 e), which correlates with the torque, experiences a similar deterioration. In contrast, the backstepping control performs well in Figures 3 a and 3 b, with more accurate tracking of the reference compared to vector control, which exhibits poor tracking performance from that moment onward. The torque (Figure 3 c) and current Iq (Figure 3 e) demonstrate favourable behaviour. Although the current Id (Figure 3 d) is slightly perturbed, it is less affected compared to vector control. These observations highlight the superior performance of backstepping control in mitigating the effects of constraints and maintaining accurate reference tracking, especially when compared to vector control.

6. Conclusion

In conclusion, this paper compared vector control (VC) and backstepping control (BC) techniques for wind systems with permanent magnet synchronous generators (PMSGs). Both techniques demonstrated distinct advantages: VC exhibited improved dynamic response and efficiency through control variable decoupling, while BC excelled in tracking performance, robustness, and disturbance rejection using a backstepping approach. The findings provide valuable insights for selecting control strategies in wind energy systems. Further research could explore hybrid approaches or optimization techniques to enhance PMSG-based wind system performance.

References

[1] F. Tahiri, A. Harrouz, Comparative Study of The Mppt Methods Applied to The PV System; Perturbation & Observation Technique, Sliding Mode Control and Fuzzy Logic Control, IEEE Xplore of 11th International Conference on Smart Grid (icSmartGrid) Paris, France, June 04-07, 2023.

[2] R. Sharma, K. Sahay, S. Singh, Control Aspects for PMSG-Based Grid-Connected Wind Energy Conversion System- A Review. SSRG International Journal of Electrical and Electronics Engineering.2023.

[3] S. Belakehal, H. Benalla, A. Bentounsi, Power maximization control of small wind system using permanent magnet synchronous generator. Journal of Renewable Energies. 2009 Jun 30;12(2):307-19.

[4] A. Harrouz, I. Colak, K. Kayisli, Energy modeling output of wind system based on wind speed. In2019 8th International Conference on Renewable Energy Research and Applications (ICRERA) 2019 Nov 3 (pp. 63-68). IEEE.

[5] I. Nouari, A. Harrouz, I. Colak, D. Beltrache, V. Dumbrava, K. Kayisli, Study and Sliding Mode Control of the Permanent Magnet Synchronous Machine, 2022 10th International Conference on Smart Grid (icSmartGrid), IEEE Xplore: 18 August 2022

[6] A. Harrouz, F. Tahiri, F. Bekraoui, and I. Boussaid, “Modelling and Simulation of Synchronous Inductor Machines”, AJRESD, vol. 1, no. 01, pp. 8-23, Jun. 2019.

[7] A. Harrouz, I. Colak, and K. Kayisli, “Control Strategy of PMSG Generator in Small Wind Turbine System”, AJRESD, vol. 4, no. 01, pp. 69-83, Jun. 2022.

[8] N. Z. Laabidine, C. El Bakkali, K. Mohammed, B. Bossoufi, Flow-oriented control design of wind power generation system based on permanent magnet synchronous generator. InInternational Conference on Digital Technologies and Applications 2021 Jan 29 (pp. 1291- 1303). Cham: Springer International Publishing.

[9] F. Bekraoui, A. Harrouz, F. Tahiri, K. Nourdine, I. Boussaid, Comparative Study Between Fuzzy Logic and PI Controller in Vector-Controlled Asynchronous Machine. InSustainable Energy-Water-Environment Nexus in Deserts: Proceeding of the First International Conference on Sustainable Energy-Water-Environment Nexus in Desert Climates 2022 Apr 26 (pp. 447-454). Cham: Springer International Publishing.

[10] Y. Bakou, L. Saihi, M. Abid, and Y. Hammaoui, “Direct Field Orientation Control Based on H∞ Method of Wind Turbine Based on DFIG ”, AJRESD, vol. 4, no. 01, pp. 111-121, Jun. 2022.

[11] F. Amin, E. B. Sulaiman, W. M. Utomo, H. A. Soomro, M. Jenal, R. Kumar, Modelling and simulation of field oriented control based permanent magnet synchronous motor drive system. Indonesian Journal of Electrical Engineering and Computer Science. 2017 May;6(2):387- 95.

[12] A. Kirad, S. Grouni, O. Mechali, Nonlinear Backstepping Control of Permanent Magnet Synchronous Motor with Rotor Speed and Position Estimation. Algerian Journal of Signals and Systems. 2018 Sep 15;3(3):133-42.

[13] A. Harrouz, H. Becheri, I. Colak, K. Kayisli, Backstepping control of a separately excited DC motor. Electrical Engineering. 2018 Sep;100(3):1393-403.

[14] M. Khatab, A. Nouh, A. S. Abd-Alraheem, A Comparative Study of Field Oriented and Backstepping Control Strategies for Wind turbine PM Synchronous Generator. International Journal of Engineering Research. 2024 Apr 1;3(1):13-32.

[15] F. Tahiri, A. Harrouz, V. Dumbrava, A. Badoud, M. Alnatoor, Non-Linear Controls For Robustness Investigation Of Pmsg-Based Wind Turbine. Upb Scientific Bulletin, Series C: Electrical Engineering And Computer Science, Politechnica University of Bucharest. 2022;84(2):377-96.

[16] K. M, Nouh, A. S. Abd-Alraheem, A Comparative Study of Field Oriented and Backstepping Control Strategies for Wind turbine PM Synchronous Generator. International Journal of Engineering Research. 2024 Apr 1;3(1):13-32.